

Supplemental data:

gp96/grp94 Chaperones GARP and Controls Functions of Regulatory T Cells

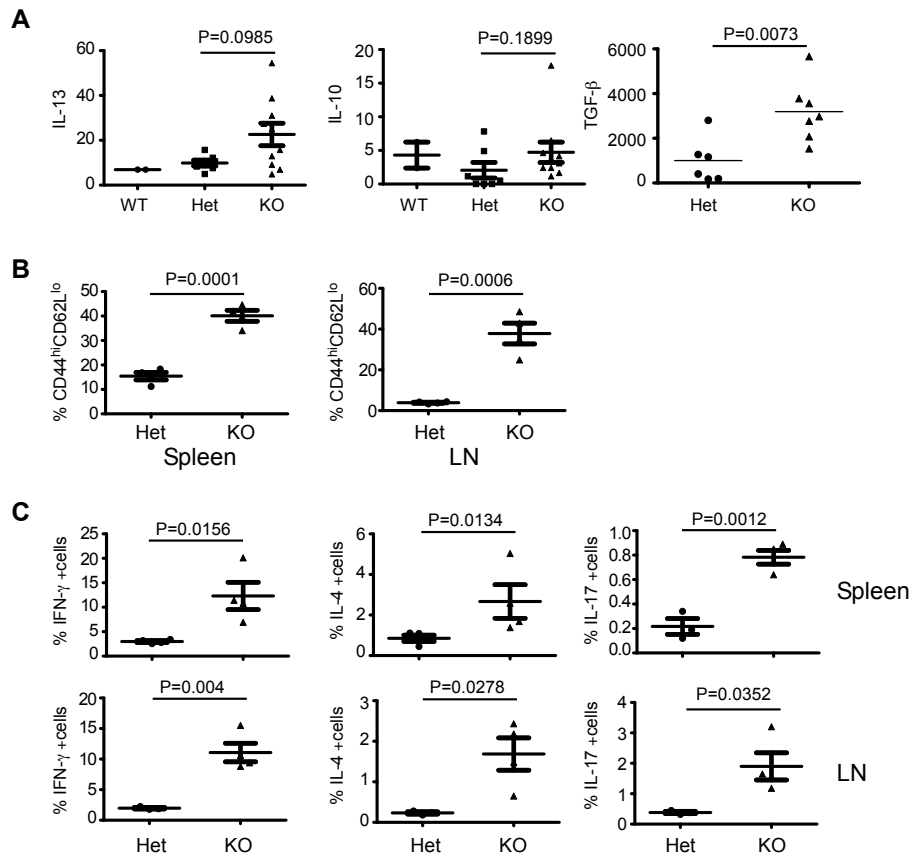
Yongliang Zhang¹, Bill X Wu¹, Alessandra Metelli¹, Jessica Thaxon¹, Feng Hong¹, Saleh Rachidi¹, Ephraim Ansa-Addo¹, Shaoli Sun², Chenthamarakshan Vasu¹, Yi Yang¹, Bei Liu¹ and Zihai Li^{1#}

¹Department of Microbiology & Immunology, Hollings Cancer Center, Medical University of South Carolina, Charleston, SC, USA

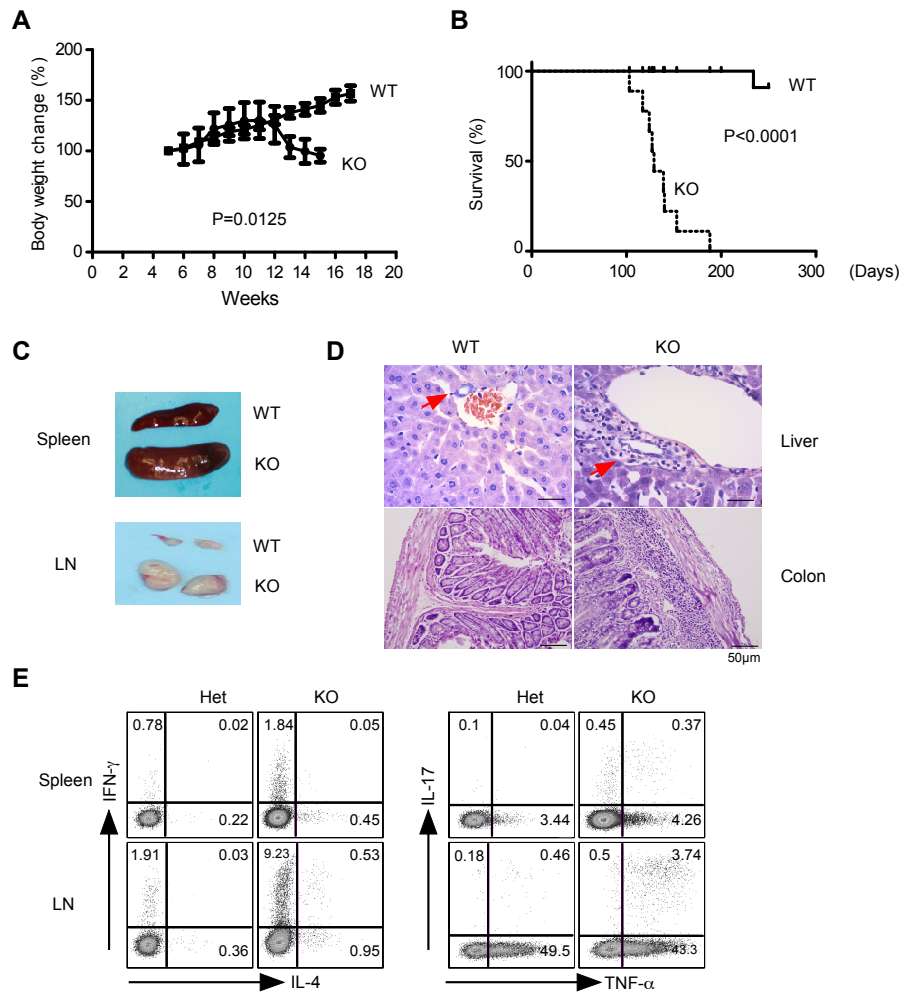
²Department of Pathology & Laboratory Medicine, Medical University of South Carolina, Charleston, SC 29425

#Corresponding author: Zihai Li, Medical University of South Carolina, 86 Jonathan Lucas Street, Charleston, SC 29425. Phone: 843-792-1034; Fax: 843-792-9588; E-mail: zihai@musc.edu

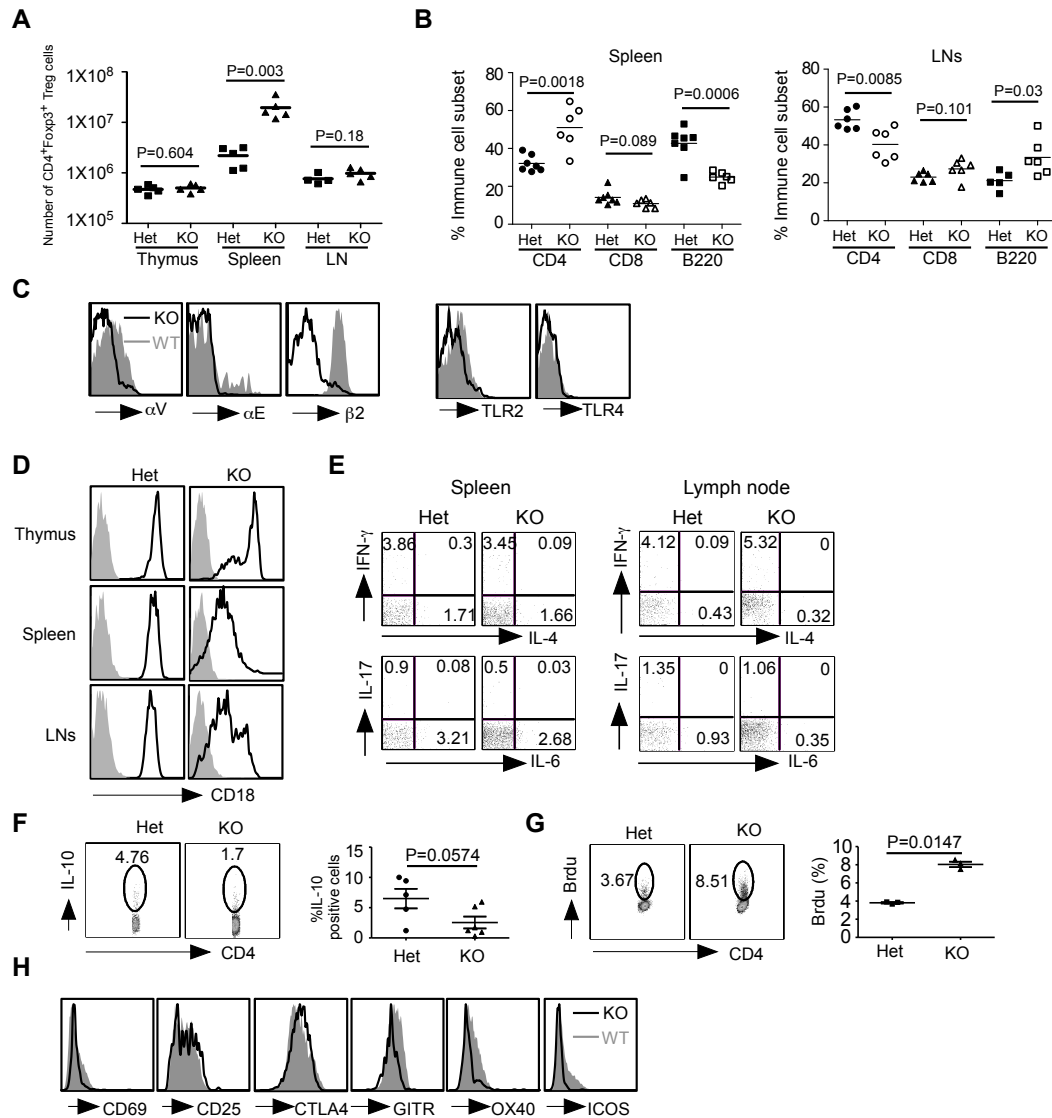
6 Figures



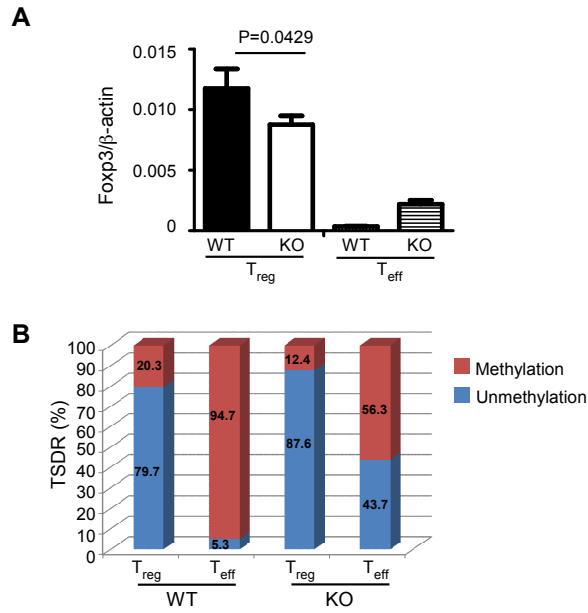
Supplement Figure 1. Uncontrolled systemic inflammatory diseases in *Hsp90b1^{flox/flox}Foxp3-EGFP^{cre}* mice. **(A)** Serum inflammatory cytokine level (pg/ml) of IL-13, IL-10, TGF-β in WT, Het and KO mice. Each dot represents value from one individual mouse. Bars: means±SEM. **(B)** Statistical analysis of CD4⁺ cells with high CD44 and low CD62L expression in 6-week-old KO mice and Het littermates. Bars: means±SEM. **(C)** Flow cytometry analysis of intracellular IFN-γ, IL-4, IL-17, IL-6 production, in response to PMA/ionomycin, by splenic CD4⁺ T cells from KO mice and Het NOD mice. Bars: means±sem. Two-tailed Student's *t* test was used for comparison of experimental groups.



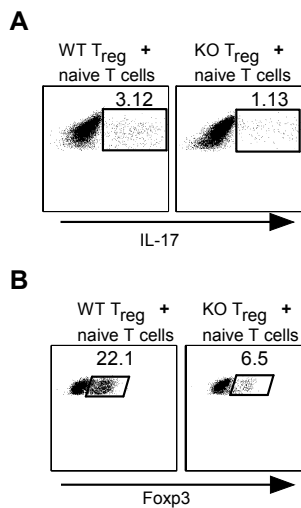
Supplement Figure 2. CD4-cre mediated deletion of gp96 in C57B/L6 mice results in systemic inflammatory diseases. (A, B) Rapid body weight loss and death of *Hsp90b^{flox/flox}CD4^{cre}* mice (n=13) compared with littermate control, *Hsp90b^{flox/wt}CD4^{cre}* (n=11). Bars (A): mean \pm sem. (C) Representative images from multiple mice demonstrate the evidence of splenomegaly and lymphadenopathy in KO mice. (D) Representative images of Haematoxylin and Eosin staining of liver and colon sections from 20-week-old *Hsp90b^{flox/flox}CD4^{cre}* and Het littermate. Scale bar: 100 μ m (colon), 50 μ m (liver). (E) Flow cytometry analysis of cytokine production intracellularly by splenic or LN CD4⁺ T cells from KO and Het littermates. Shown are representative data from two independent experiments. Statistic difference of body weight change in (A) was confirmed with two-way ANOVA, and mouse survival differences in (B) were analyzed with log-rank (Mantel-Cox) test.



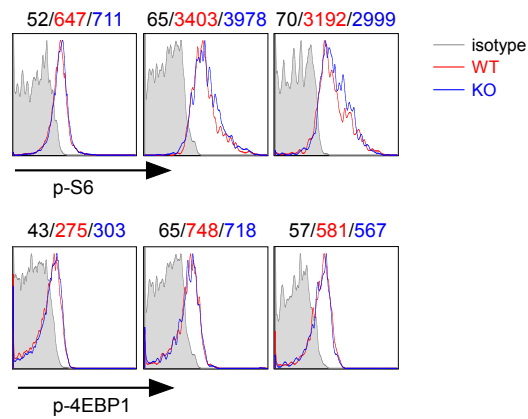
Supplement Figure 3. Characterization of T_{reg} cells and other subsets of immune cells in mice with T_{reg}-specific deletion of gp96. (A) Absolute T_{reg} cell number in different immune organs. Bar: mean ± sem. (B) Immune cell subset distribution in the spleen and lymph node. Bar: mean ± sem. (C) Flow cytometry analysis of indicated cell surface integrins and TLRs of T_{reg} cells from *Hsp90^{fllox/fllox} Foxp3-EGFP^{cre}* mice and WT littermate. Data represent two independent experiments. (D) Flow cytometry analysis of CD18 expression by CD4⁺Foxp3⁺ cells from thymus, spleen and Lymph nodes. (E) Flow cytometry analysis of intracellular IFN-γ, IL-4, IL-17 and IL-6 expression by CD4⁺Foxp3⁺ T cells from the spleen and LNs. Numbers represent percentage of cells in each quadrant. Data represent three independent experiments. (F). Flow cytometry analysis of intracellular IL-10 expression (%) by CD4⁺Foxp3⁺ T cells from spleen and LNs. (G) Flow cytometric analysis of BrdU incorporation (%) by Het and KO CD4⁺Foxp3⁺ T cells from the spleens. (H) Flow cytometric analysis of splenic T_{reg} cells for the indicated cell surface markers from bone marrow chimeric mice transplanted with 1:1 mixture of CD45.2⁺ WT and CD45.1⁺ KO bone marrows. Data represent three independent experiments. The two-tailed Student's *t* test was used for comparisons between Het and KO mice.



Supplement Figure 4. Quantification of *Foxp3* mRNA expression level and *Foxp3* promoter methylation status. CD4⁺CD25⁺ T_{reg} cells and CD4⁺CD25⁻ T effector cells were isolated by MACS beads followed by isolation of mRNA and genomic DNA. **(A)** Quantification of *Foxp3* mRNA by q-RT-PCR. Data represent two independent experiments. Two-tailed Student's *t* test were used for comparisons between WT and KO mice. **(B)** DNA demethylation in the TDSR region was quantified with demethylation-specific probe by the Taqman Real time-PCR as described in Materials and Methods. Four independent experiments were performed with similar findings. Data represent mean ± sem (A) and mean (B).



Supplement Figure 5. Compromised activity of gp96 KO T_{reg} cells in driving T_{h17} cells and iT_{reg} cell differentiation *in vitro*. (A, B) CD4⁺CD25⁺ T_{reg} cells were activated with plate bound anti-CD3 antibody (2 μg/ml) for 2-3 days, followed by irradiation (2000 cGy) and co-culturing with CFSE-labeled CD4⁺CD25⁻ naïve T cells for 3 days, in the presence of anti-CD3 antibody and IL-2 for T_{reg} cells, and additional IL-6 for T_{h17} cells as described in Materials and Methods. Intracellular staining of IL-17 and Foxp3 were performed, followed by flow cytometry. Data represent more than three independent experiments.



Supplement Figure 6. gp96-deficient T cells exhibit normal mTORC1 activity. Phosphorylation of p-S6 (upper panel) and 4E-BP1 (lower panel) in freshly isolated naïve T cells (CD4⁺CD44^{low}Foxp3⁻, Left), T_{reg} cells (CD4⁺Foxp3⁺, Middle), and memory-phenotype (MP) T cells (CD4⁺CD44^{high}Foxp3⁻, Right). Numbers above the plots indicate mean fluorescent intensity (MFI). Two independent experiments were performed with similar findings.